

# Exploring Crack Reduction in High-Performance Concrete: The Impact of Nano-Silica, Polypropylene, and 4D Metallic Fibers

Mohammadfarid Alvansazyazdi <sup>a,b,c\*</sup>, Diego Farinango <sup>b</sup>, Javier Yaucan <sup>b</sup>, Alexander Cadena <sup>b</sup>, Jorge Santamaria <sup>b</sup>, Pablo M. Bonilla-Valladares <sup>d</sup>, Mario Leon <sup>b</sup>, Alexis Debut <sup>e</sup>, Mahdi Feizbahr <sup>f</sup>, Luis Leon <sup>b,g</sup>, Byron Ayala <sup>b</sup>

<sup>a</sup> Institute of Science and Concrete Technology, ICITECH, Universitat Politècnica de València, Spain.

<sup>b</sup> Faculty of Engineering and Applied Sciences, Civil Engineering Department, Central University of Ecuador, Av. Universitaria, Quito 170521, Ecuador.

<sup>c</sup> Faculty of Engineering, Industry and Construction, Civil Engineering Department, Laica Eloy Alfaro de Manabi University, Manabi Manta, Ecuador.

<sup>d</sup> Faculty of Engineering and Applied Sciences, School of Civil Engineering, Central University of Ecuador, Av. Universitaria, Quito 170521, Ecuador.

<sup>e</sup> Department of Life Sciences and Agriculture, Center for Nanoscience and Nanotechnology, University of the Armed Forces ESPE, Sangolquí 171103, Ecuador.

<sup>f</sup> School of Civil Engineering, Engineering Campus, University Sains Malaysia, Nibong Tebal, Penang, Malaysia.

<sup>g</sup> Benito Juárez University, 36th Street Nte. 1609, Christopher Columbus, 72330 Heroic Puebla de Zaragoza, Pue., Mexico.

## Article Information

### Article History

Received: 11/12/2023

Accepted: 16/05/2024

Available online: 20/05/2024

### Keywords

Concrete,  
Nano-silica,  
Polypropylene fiber,  
Steel fiber,  
Contraction,  
Evaporation,  
Crack reduction ratio (CRR)

## Abstract

By contrasting plain concrete, high-performance concrete (HPC) with nano-silica, high-performance concrete with polypropylene fiber addition, and high-performance concrete with 4D metallic fiber addition, this work aims to verify crack control. Getting data on the mechanical and physical characteristics of pure concrete is the first stage in the process. The HPC mixes and the HPC mixtures with fiber addition will next be evaluated in a "air chamber," a controlled environment device built in accordance with ASTM C-1579-13 requirements. In order to guarantee accurate findings for getting fractures due to plastic shrinkage—which happens when the evaporation rate surpasses 1 kg/m<sup>2</sup>/h—these mixes will be tested for six hours under predetermined ambient conditions. As a result, there is more surface evaporation of water than there is inward concrete water exudation. The concrete will be exposed to crack formation and evaluated both qualitatively through visual observation and quantitatively by calculating the Crack Reduction Ratio (CRR), which will be expressed as a percentage and will show how effective the fiber types used.

## 1. Introduction

The mortar has played a fundamental role in construction throughout history. As described by Chudley and Greeno (2006), this material has been an essential component for bonding a variety of elements, such as bricks, stones, and blocks. In recent years, the increase in the use of structural masonry and its impact on the construction of civil works, particularly in buildings, has led to a significant rise in

\* Corresponding author: Institute of Science and Concrete Technology, ICITECH, Universitat Politècnica de València, Spain.

E-mail address: [faridalvan@uce.edu.ec](mailto:faridalvan@uce.edu.ec)

the demand for mortar, both for bonding and for plastering or rendering. However, unlike concrete, which has well-established protocols for its production, specific technical design and quality control procedures for mortar have not yet been developed, representing a challenge in ensuring its excellence in modern constructions (Feizbahr et al., 2013; Rivera, 2009).

Contraction is the process that concrete undergoes during curing and drying. It is primarily due to the evaporation loss of excess water during the mixing process. In fact, it is the shortening of the concrete (shrinkage) that occurs during the hardening process (Kovler & Lange, 2004). Concrete shrinks as it loses moisture through evaporation. However, the deformation caused by shrinkage has no effect on the tensile stress acting on the concrete. This phenomenon can be easily observed when cracks appear on the surface of dried concrete. Shrinkage can largely be a reversible phenomenon if appropriate curing methods are used, such as saturation after shrinkage, which causes the structure to expand until it reaches almost its original volume. In this regard, shrinkage is an apparently simple phenomenon in concrete when it loses water. Strictly speaking, shrinkage is a three-dimensional deformation, but it is expressed as linear deformation because in most exposed concretes, one or two dimensions are much smaller than the third, and the effect of shrinkage is greater in the larger dimension (Asli & Arabani, 2022; Sosa, 2018). According to Becker (2021), in common language, dry shrinkage is an abbreviation of the term "drying shrinkage" in cured concrete exposed to an environment with a relative humidity lower than 100%.

Vallejo (2020) states that there are several types of shrinkage that can occur simultaneously or independently, depending on the conditions. For the purposes of this research, the focus is on plastic shrinkage, which occurs when fresh concrete loses moisture after finishing and before gaining strength. The extent of this shrinkage depends on air temperature, relative humidity, concrete temperature, and wind speed (Vallejos, 2020). On the other hand, nano-silica is a liquid additive derived from amorphous silica micro-particles ( $\text{SiO}_2$ ). Nano-silica particles have a smaller size, high purity and reactivity, as well as a crystalline structure similar to that of silica fume, which is expected to yield better results (Alvanzas & Bombon, 2022; Mukharjee & Barai, 2015; Oh et al., 2021; Prusty et al., 2015).

It is a liquid nano-additive, which has a turbid and slightly viscous appearance, and is composed of silica with nanoparticle size. It is an excellent water-reducing agent with high potency and pozzolanic activity. Currently, nano-silica is used as a supplementary material in civil engineering and other industries to produce environmentally friendly concrete mixes, where a certain percentage of cement is replaced by another material, such as silica fume or calcium silicate hydrate (Alvansazyazdi et al., 2023; Budenberg, 2021; S. Ferdosi & Porbashiri, 2022; García-Taengua et al., 2015; Wu & Cui, 2023). The addition of nano-silica to concrete mixes offers several significant benefits, particularly regarding the modulus of elasticity. It provides the material with the necessary properties to ensure watertightness, workability, and compaction (García-Taengua et al., 2015; Hosseini & Toghroli, 2021; Sánchez & Bernal, 2018). From an environmental standpoint, the use of this additive reduces the amount of  $\text{CO}_2$  released into the environment during cement production, as a significant portion of this component is replaced by silica fume particles obtained from industrial waste from various industries worldwide. Furthermore, the incorporation of nano-silica in concrete aims to achieve high-performance concrete, as it requires lower amounts of water, resulting in reduced shrinkage effects as observed through laboratory experimentation (Feizbahr et al., 2013; S. B. Ferdosi, 2022; Mukharjee & Barai, 2019; Toosi & Ahmadi, 2023; Yang et al., 2019). The "contact zone" between aggregates can be improved by using nanoparticles, leading to a better bond between the cement paste and aggregates. Additionally, nanoparticles offer advantages such as crack prevention and interlocking effects between slip planes, which enhance the hardness, shear, tensile, and flexural strength of cement-based materials.

Furthermore, nanoparticles have the ability to act as nano-reinforcement, strengthening the tensile strength of concrete(Alvansaz & Rosero, 2019; Feizbahr et al., 2020). However, the use of nano-silica additives in any type of concrete should be carried out by specialists with the appropriate knowledge. Otherwise, there is a risk of deteriorating the properties of the material, which jeopardizes the safety and stability of the construction. According to the scientific article "Prevention of pollution in concrete manufacturing through the use of silica nanoparticles," the results obtained from incorporating 2.0% silica nanoparticles into conventional concrete show a significant improvement in its mechanical properties(Alvansaz et al., 2020).

**Table 1.** Aggregate Tests

<b>CHARACTERISTIC TESTS OF MATERIALS AND CONCRETE</b>	
<b>TEST</b>	<b>STANDARD NTE INEN</b>
<b>COARSE AGGREGATE</b>	
Específico Real Density Specific Weight	NTE INEN 857- 2010
Absorption Capacity	NTE INEN 857- 2010
Unit Mass	NTE INEN 858- 2010
Optimum Density	NTE INEN 858- 2010
Particle Size Distribution	NTE INEN 696- 2011
Abrasion	NTE INEN 860- 2011
Moisture Content	NTE INEN 862- 2011
<b>FINE AGGREGATE</b>	
Colorimetry	NTE INEN 855- 2010
Real Density Specific Weight	NTE INEN 856- 2010
Absorption Capacity	NTE INEN 856- 2010
Unit Mass	NTE INEN 858- 2010
Optimum Density	NTE INEN 858- 2010
Particle Size Distribution	NTE INEN 696- 2011
Moisture Content	NTE INEN 862- 2011

*Note:* The table shows the types of tests used for the research work

## 2. Materials and Methods

### 2.1. Method

For the development of the research, the hypothetical demonstrative method has been employed. Through this method, it was determined that high-performance concrete (HPC) incorporating nano-silica particles can exhibit improved properties and a higher resistance to contraction during implementation. Furthermore, the materials used in the research were fine and coarse aggregates, which were selected based on their ease of acquisition and frequent use in construction in the city of Quito.

To study high-performance concrete, an analysis was conducted on the behavior of the fine and coarse aggregates with nano-silica, as well as with 4D steel fibers and polypropylene fibers in fresh concrete. The aim was to provide valuable information in the field of concrete. In the preparation of the concrete specimens, various characteristic tests were performed on fresh concrete following the NTE INEN (Ecuadorian Technical Standard) and ASTM (American Society of Testing Materials) standards.

## 2.2. Granulometric Test

The granulometric test is based on the NTE INEN 969 standard, which aims to determine the particle size distribution of fine and coarse aggregates through a sieving process. This method utilizes a series of sieves arranged in order of decreasing opening size, through which the material passes and is retained based on the particle size. To calculate the reference granulometric curve of the coarse and fine aggregate, formulas were used, from which the granulometric curves are obtained:

### Coarse Aggregate Fineness Modulus:

$$MF = \frac{\sum \% \text{Cumulative Retained} (1 \frac{1}{2} + \frac{3}{4} + \frac{3}{8} + \text{No. 4} + \text{No. 8} + \text{No. 16} + \text{No. 30} + \text{No. 50} + \text{No. 100})}{100}$$

$$\text{Fineness Modulus (MF)} = 6.462$$

$$\text{Maximum Nominal Size} = 3/4''$$

### Fine Aggregate Fineness Modulus:

$$MF = \frac{\sum \% \text{Cumulative Retained} (\frac{3}{8} + \text{No. 4} + \text{No. 8} + \text{No. 16} + \text{No. 30} + \text{No. 50} + \text{No. 100})}{100}$$

$$\text{Fineness Modulus (MF)} = 3.406$$

## 2.3. Design Parameters

In order to obtain high-performance concrete capable of resisting cracking under controlled ambient conditions, compression strength tests have been conducted using test specimens, and for shrinkage, trays were tested in the controlled environment machine.

### 2.4. Design Procedure for Proportioning

There are no standardized methods for the design of high-performance concrete. Therefore, for this research, the design was based on the results of scientific investigations as recommended by ACI 211.4R-08. The mixture design involves following a protocol based on the design methodology described by the maximum density of aggregates method.

### 2.5. Mix Design with 2% Nano-silica Replacement of Cementitious Material

Based on the standard mix design, a mix design is developed with a 2% substitution of nano-silica as a cementitious material for the subsequent determination of aggregate volumetrics.

**Table 2.** Mix Design with 2% Nano-silica Replacement of Cementitious Material

DESCRIPTION	QUANTITY	UNIT
Cement	382.78	Kg
Water	156.24	Kg
Nanosilica	7.81	Kg
Ratio w/c	0.4	-
Air Content	2.5	%

*Note.* The table shows the proportioning of the standard mix.

### 2.6. Volume Proportioning for Steel and Polypropylene Fibers

The amount of fiber is added based on the volume of concrete, using a simple proportion rule with the recommendation from the technical datasheets. Steel fibers 4D: It is recommended to use 10 kg per  $m^3$  and polypropylene fibers 1 kg per  $m^3$

### 2.7. Mixing Procedure

As it is a special concrete with materials like nano-silica, a specific mixing methodology is necessary to ensure proper adhesion of the nano-silica nanoparticles in the mix. It is recommended to reserve a minimum amount of water to dissolve the nano-silica in a homogeneous mixture, as indicated in the following image, in addition to the water used to dissolve the superplasticizer additive, which improves workability in the mix. It is advised to add the homogenized nano-silica mixture after the mixing of the fine and coarse aggregates.

After mixing, the mixture is poured into molds that meet the requirements of the ASTM C 1579-13 standard. These molds are then placed in a controlled environment chamber. The settlement flow is measured according to the ASTM C 1611 standard, and the mixture is transferred into cylindrical specimens for compression testing.



**Figure 1.** Pouring of the nano-silica mixture into the mix.



**Figure 2.** Placement of the mixture on the vibrating table for 10 seconds to achieve leveling and smoothing.

### 2.8. Air Chamber Test for Shrinkage Testing.

The equipment used for the shrinkage test complies with the technical specifications of the ASTM C-1579-13 standard.

The controlled environment of the testing chamber must simulate the following conditions:

- Severe climatic conditions with a temperature of  $36^{\circ}\text{C} \pm 3^{\circ}\text{C}$ .
- Air outlet velocity (wind) between 4.8 to 5.2 m/s.
- Relative humidity between 20% and 40%.
- Evaporation rate greater than 1 kg/m<sup>2</sup>/h.

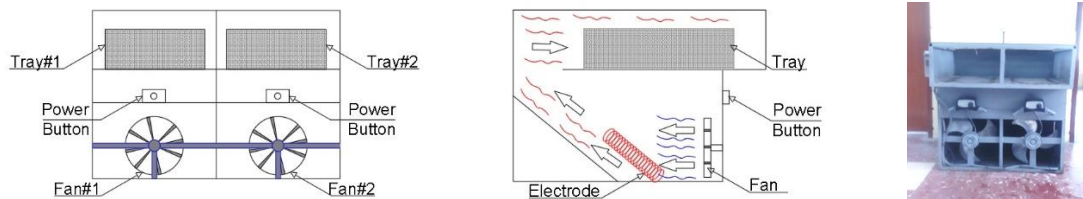


**Figure 3.** Controlled Environment Chamber and Temperature Control

Wind speed is determined using an anemometer, which is measured by a fan-type sensor that reacts to the presence of air currents. For relative velocity, we use a hydrometer that measures the constant ambient temperature and the humidity present in the environment. The rate of evaporation is determined using a water container.



**Figure 4.** Anemometer and Hydrometer measuring wind speed and humidity, respectively.

### 3. Results

Based on the results obtained from the laboratory mixes, including the control mix and the substitution of cementitious material with nano-silica, as well as the incorporation of steel fibers and polypropylene fibers, a comparative analysis of their mechanical and physical properties will be conducted to assess the effect of these materials on conventional concrete.

#### 3.1. Results of Physical Properties

In the visual analysis, the slump values ranged between 9 and 12 cm, indicating wet concrete and achieving good workability. This workability was obtained by using different dosage percentages of the superplasticizer MASTERGLENIUM 7955, which improved cohesion and reduced segregation until the appropriate amount of additive was determined to achieve excellent cohesion without segregation in the mix. The variation in the percentage of superplasticizer depends on the adsorption capacity of the aggregates, cement, nano-silica, and the fiber addition percentage (Table 3).

**Table 3.** Results of Physical Properties

MIXTURE	PROPERTIES				
	As (cm)	Consistency	Workability	Cohesion	Segregation
Standard Mix	10.5	Wet	Good	Good	Low
2% Nanosilica	10	Wet	Good	Good	Low
2% Nanosilica +10% Steel fibers	9.5	Wet	Good	Good	Low
2% Nanosilica +1% Polipropylene fibers	9	Wet	Good	Good	Low

*Note:* The table presents the dosage of the control mix.

#### 3.2. Results of Mechanical Properties

- **Compressive Strength Results**

The overall results of the compression tests are presented, showing the average strength values obtained at the ages of 7, 14, and 28 days. The percentages achieved by each mixture in relation to the required strength are also provided.

**Table 4.** Compressive Strength Results at 7, 14, and 28 days

DAYS	Cylinder #	Standard	Nanosilica	Nanosilica	
				Polyp.	Nano-silica
		MPa	MPa	MPa	MPa
7	1	37.85	42.64	43.57	44.60
	2	37.37	43.00	43.97	45.63
	3	37.56	42.80	44.60	45.96
14	1	45.57	48.56	50.78	52.75
	2	45.01	49.00	51.09	52.98
	3	46.60	48.97	50.80	53.10
28	1	50.15	53.58	54.76	58.02
	2	49.80	52.61	54.65	57.90
	3	50.27	52.86	54.90	58.52

*Note.* The table shows the results of strength.

In Table 5, the average results are presented for the preparation of the compressive strength vs. time graph.

**Table 5.** Average Results of Compressive Strength at 7, 14, and 28 days

T	MP	MN	N+FP	N+FS
7	37.60	42.81	44.04	45.40
14	45.73	48.84	50.89	52.94
28	50.07	53.02	54.77	58.15

*Note.* The table shows the average resistance result.

The results obtained from the compressive strength test allow us to identify that the substitution of a percentage of cementitious material with nano-silica additions, along with the addition of polypropylene fibers and steel fibers, yields a positive result by improving the compressive strength compared to the control mix. In the Stress-Strain vs. Time graph (Figure 5), the behavior of the different mixes is exemplified as their age increases. It can be observed that the curve of the concrete mix with nano-silica + steel fibers exhibits higher compressive strength compared to the control mix.

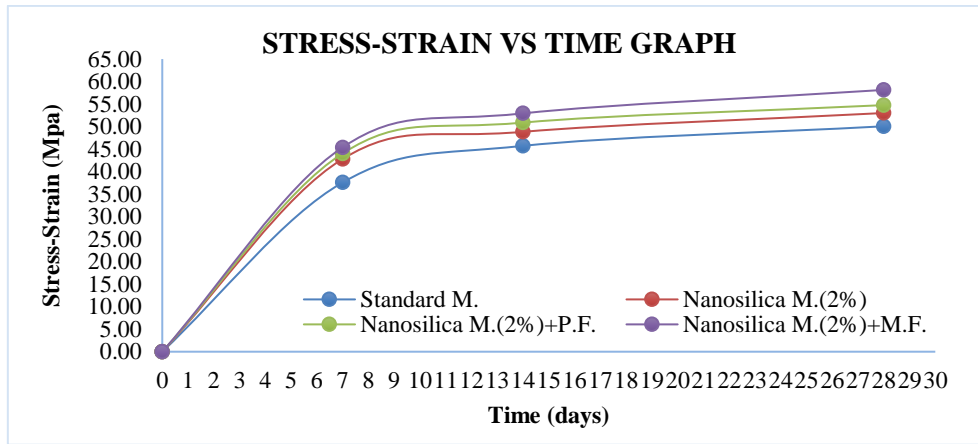


Figure 5. Stress-Strain Vs Time Graph

The compressive strength illustration clearly shows that the values obtained for the nano-silica mixture yield positive results for each addition. The concrete mixture with a 2% addition of nano-silica and metal fibers achieved higher strength, with a value of 58.15 MPa at 28 days.

### 3.3. Analysis and Interpretation of Results for Shrinkage Test

To analyze the effect on shrinkage in high-performance concrete with nano-silica and steel 4D fibers, as well as polypropylene fibers, a quantitative description of the degree of cracking due to plastic shrinkage of the concrete was performed.

- **Quantitative Analysis of Plastic Shrinkage**

For an accurate shrinkage analysis, proper handling of specimens in the controlled environment chamber is necessary.

- The test was conducted for six hours in the air chamber.
- Wind speed should be greater than 4.7 m/s.
- Temperature:  $36^{\circ}\text{C} \pm 3^{\circ}\text{C}$ .
- Relative humidity:  $30\% \pm 10\%$ .
- Evaporation rate ranging from 1.43 to 1.88  $\text{kg}/\text{m}^2/\text{h}$ , which should be higher than 1  $\text{kg}/\text{m}^2/\text{h}$  according to the standard.

Afterward, the crack width is measured on the short side of the panel at every 10mm along the entire length of the crack, leaving a distance of 25mm from the mold edge towards the center at both ends. Cracks observed at the panel's ends are not considered as they are caused by the mold edge effect.

To measure the cracks, a crack gauge card (Figure 6) with a precision of 0.05mm is used. The measurement is performed twice to obtain a more accurate result. Cracking in conventional concrete occurred four hours after being placed in the air chamber, while in steel fiber-reinforced concrete, it occurred two hours and twenty minutes after placement.



Figure 6. Crack Comparator Card

- **Scale for measuring crack widths (mm)**

To perform the scaling of the crack gauge according to the article "Ciencia y Sociedad de la República Dominicana" and the crack comparator card provided by SIKA, the process involved obtaining lines with thicknesses ranging from 0.05 to 2.60mm. The precision of the crack gauge is 0.05mm, as described in ASTM C 1579-13 standard. The methodology for measuring the widths of concrete cracks involves sliding the prepared scale card until it aligns with the width of the concrete crack.

- **Determination of Crack Reduction Ratio (CRR)**

The Crack Reduction Ratio (CRR), determined by ASTM C-1579-13 standard, aims to assess the percentage reduction of cracks between concrete samples with the addition of both metallic and polypropylene fibers and control samples. It is calculated as shown in the equation below.

$$CRR = \left[ 1 - \frac{\text{Average Width of Cracks in Fiber – Reinforced Concrete}}{\text{Average Width of Cracks in Control or Conventional Concrete}} \right] \times 100\%$$

- **Average crack width using the statistical method of frequencies**

Below are the values obtained in the test (Table 1, 2, 3), from which an analysis of crack width distribution was conducted using the statistical method of frequencies to determine the number of occurrences of the data and to consider the highest concentration of crack widths by removing highly scattered values, i.e., very small or very large cracks. The following steps are followed for this purpose:

- The values from the tables are taken to determine the number of data points, lower limit, upper limit, range, number of classes, and width in order to establish crack width intervals for each water-cement ratio.
- Next, the analysis of crack width distribution is performed, considering only the values with the highest frequency concentration.
- Once the crack width analysis is obtained, the crack widths from the original test data are selected.
- The average crack width is calculated using only the analyzed crack widths.
- Then, the Crack Reduction Ratio (CRR) percentage is calculated using the equation, for a water-cement ratio of W/C=0.40.

**CRR1      61      %**

**CRR2      66      %**

The Crack Reduction Ratio (CRR) ranges from 0 to 100%, where 0% indicates complete cracking and 100% represents concrete without any cracks. In the case of concrete with steel fibers, it exhibits a crack resistance between 61% and 66%.

**CRR1      70      %**

**CRR2      73      %**

The CRR (Crack Reduction Ratio) ranges from 0% to 100%, where 0% signifies complete cracking and 100% represents concrete without any cracks. In the case of concrete with polypropylene fibers, it exhibits a crack resistance of approximately 70% to 73%. The inclusion of polypropylene fibers in concrete improves its crack resistance since these fibers tend to align and accommodate themselves better during the curing process among the aggregates.

**Table 6.** Summary of direct costs and compressive strength

Mix Type	28-Day Strength	Price/m <sup>3</sup>
Standard Mix	50.072	\$ 123.75
Optimum Mix 2% Nano-silica	53.019	\$ 234.36
Optimum Mix + Polypropylene Fibers	54.770	\$ 247.86
Optimum Mix + 4D Steel Fibers	58.147	\$ 253.40

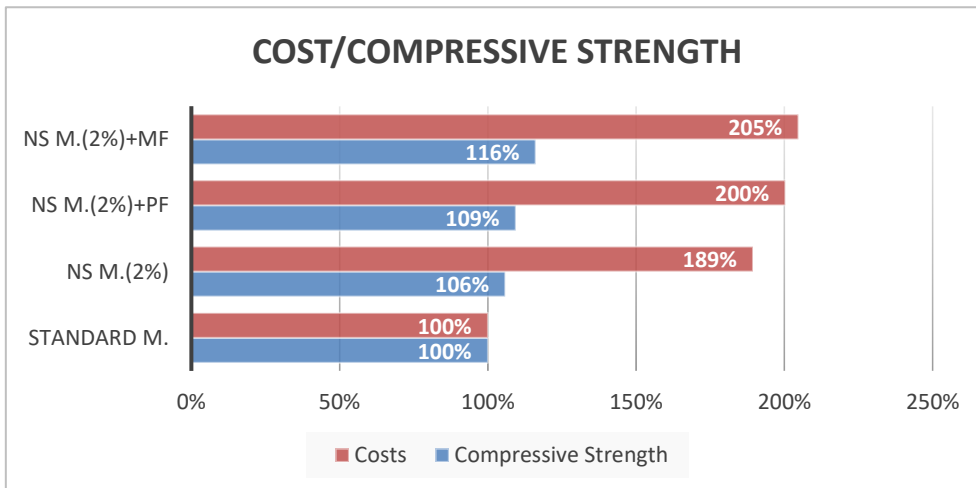


**Figure 7.** Manufacturing cost for each nano-silica addition.

#### 4. Conclusions

The undoped high-strength concrete (composed of sand, gravel, cement, water, and no additives) exhibits its first crack, as detected by visual inspection, at the fourth hour of being subjected to the air chamber test, with a maximum crack width of 0.508mm. When evaluating a high-performance concrete (HPC) with 2% replacement of cement by weight with nano-silica in the air chamber test, cracking is observed at the fourth hour, plus an additional 30 minutes of testing in the air chamber. At the end of the test, it exhibits a maximum crack width of 0.356mm. The indicator of the efficiency of using fibers in concrete to counteract cracks is known as the Crack Reduction Ratio (CRR), as determined by ASTM C-1579-13 standard. This standard relates the cracks in fiber-reinforced concrete to the cracks in concrete without fibers or any additives, and it is expressed as a percentage. The use of polypropylene fibers in high-performance concrete (HPC) exhibits an average Crack Reduction Ratio (CRR) of 72%, indicating a significant reduction in cracks. On the other hand, the use of 4D steel fibers shows a CRR value of 64%. It should be noted that a value close to 100% implies no cracking. Therefore, both polypropylene and steel fibers are effective in reducing cracks, with polypropylene fibers demonstrating a slightly higher efficiency in crack reduction.

The research indicates that the use of polypropylene fibers, with a lower weight but a higher volume compared to steel fibers, creates an interconnected network resembling a neural network. This network structure hinders cracking due to plastic shrinkage. The increased volume of polypropylene fibers allows for more interlocking and bonding within the concrete matrix, providing enhanced crack resistance. This phenomenon contributes to the effectiveness of polypropylene fibers in reducing cracks and improving the overall performance of the concrete. The use of 4D steel fibers exhibits higher compressive strength compared to concrete with polypropylene fibers, highlighting the importance of the shape and arrangement of the fibers in the mixture for effectiveness based on the specific physical and mechanical requirements of the concrete. The structural properties of steel fibers, such as their high tensile strength and stiffness, contribute to the overall strength of the concrete and enhance its load-bearing capacity. The choice of fiber type, whether steel or polypropylene, should be determined based on the desired physical and mechanical characteristics of the concrete, taking into account factors such as the intended application and the specific performance requirements.

#### Declaration of conflicting interests

The authors declare that they have no competing financial interests or personal relationships that could have influenced the information presented in this article.

#### Acknowledgments

We would like to express our gratitude to Alexis Debut from the Center for Nanoscience and Nanotechnology at Armed Forces University ESPE for his invaluable assistance, as well as to the laboratory team. Furthermore, we appreciate the support from the INECYC staff and the material testing laboratory at the Central University of Ecuador.

#### References

- Alvansaz, M., Morales, L., Landázuri, P., & Vásconez, W. (2020). Prevention of pollution in concrete manufacturing through the use of silica nanoparticles. *RISTI*, 309-324.
- Alvansaz, M., & Rosero, J. (2019). The pathway of concrete improvement via nano-technology. *INGENIO*, 2(1), 53.

- Alvansazyazdi, M., Alvarez-Rea, F., Pinto-Montoya, J., Khorami, M., Bonilla-Valladares, P. M., Debut, A., & Feizbahr, M. (2023). Evaluating the Influence of Hydrophobic Nano-Silica on Cement Mixtures for Corrosion-Resistant Concrete in Green Building and Sustainable Urban Development. *Sustainability*, 15(21), 15311.
- Alvanzas, M., & Bombon, C. (2022). Estudio de la Incorporación de Nano Sílice en Concreto de Alto Desempeño (HPC). *INGENIO*, 5(1), 12-21.
- Asli, H. H., & Arabani, M. (2022). Analysis of Strain and Failure of Asphalt Pavement. *Computational Research Progress in Applied Science & Engineering*, 8(01).
- Becker, E. (2021). *Pisos industriales de hormigón: Diseño, construcción y mantenimiento*: Nobuko.
- Budenberg, E. (2021). Amorphous micro and nano silica extracted from rice husk and obtained by acidic prehydrolysis and calcination: Ipreparation route and characterization. *Imagem da Capa Kateryna Kon*, 1(1), 67-76.
- Chudley, R., & Greeno, R. (2006). *Building construction handbook*: Routledge.
- Feizbahr, M., Jayaprakash, J., Jamshidi, M., & Keong, C. (2013). Review on various types and failures of fibre reinforcement polymer. *Middle-East Journal of Scientific Research*, 13(10), 1312-1318.
- Feizbahr, M., Mirhosseini, S. M., & Joshaghani, A. H. (2020). Improving the performance of conventional concrete using multi-walled carbon nanotubes. *Express Nano Letters*, 1, 1-9.
- Ferdosi, S., & Porbashiri, M. (2022). Calculation of the Single-Walled Carbon Nanotubes' Elastic Modulus by Using the Asymptotic Homogenization Method. *International Journal of Science and Engineering Applications*, 11(12), 254-265.
- Ferdosi, S. B. (2022). Thermal Effect on The Post-buckling And Mechanical Response of Single-Walled Carbon Nanotubes: A Numerical Investigation. *Mechanical Engineering*, 9, 1-6.
- García-Taengua, E., Sonebi, M., Hossain, K., Lachemi, M., & Khatib, J. (2015). Effects of the addition of nanosilica on the rheology, hydration and development of the compressive strength of cement mortars. *Composites Part B: Engineering*, 81, 120-129.
- Hosseini, S. A., & Toghroli, A. (2021). Effect of mixing Nano-silica and Perlite with pervious concrete for nitrate removal from the contaminated water. *Advances in concrete construction*, 11(6), 531.
- Kovler, K., & Lange, D. (2004). Cracking Risk Associated with Early Age Shrinkage. Cement. *Cement and Concrete Composites*, 26(5), 521-530.
- Mukharjee, B. B., & Barai, S. V. (2015). Characteristics of sustainable concrete incorporating recycled coarse aggregates and colloidal nano-silica. *Advances in concrete construction*, 3(3), 187.
- Mukharjee, B. B., & Barai, S. V. (2019). Performance assessment of nano-Silica incorporated recycled aggregate concrete. *Advances in concrete construction*, 8(4), 321.
- Oh, T., You, I., Banthia, N., & Yoo, D.-Y. (2021). Deposition of nanosilica particles on fiber surface for improving interfacial bond and tensile performances of ultra-high-performance fiber-reinforced concrete. *Composites Part B: Engineering*, 221, 109030.
- Prusty, R., Mukharjee, B. B., & Barai, S. V. (2015). Nano-engineered concrete using recycled aggregates and nano-silica: Taguchi approach. *Advances in concrete construction*, 3(4), 253.
- Rivera, G. (2009). Tecnología del concreto y mortero. *Ciudad del Cauca: Universidad del Cauca*, 235.

- Sánchez, E., & Bernal, J. (2018). Propiedades reológicas y mecánicas de un hormigón autocompactante con adición de nano-sílice y micro-sílice. *Revista ALCONPAT*, 6(1), 1 - 14.
- Sosa, M. (2018). *Estudio de la contracción por secado en morteros y hormigones con agregados finos reciclados*. Retrieved from La Plata:
- Toosi, G., & Ahmadi, M. M. (2023). *Robust Process Capability Indices for Multivariate Linear Profiles*. Paper presented at the 2023 Systems and Information Engineering Design Symposium (SIEDS).
- Vallejos, C. (2020). Hormigón reforzado con vidrio molido para controlar grietas y fisuras por contracción plástica. *Pro Sciences: Revista de Producción, Ciencias e Investigación*, 4(31), 31-41.
- Wu, J., & Cui, Y. (2023). Improving the concrete quality and controlling corrosion of rebar embedded in concrete via the synthesis of titanium oxide and silica nanoparticles. *Advances in concrete construction*, 15(1), 1.
- Yang, L., Shi, C., & Wu, Z. (2019). Mitigation techniques for autogenous shrinkage of ultra-high-performance concrete—A review. *Composites Part B: Engineering*, 178, 107456.